Vibrational Optical Activity of (3*S*,6*S*)-3,6-Dimethyl-1,4-dioxane-2,5-dione

Cheok N. Tam,[†,‡] Petr Bour,[§] and Timothy A. Keiderling*[,†]

Contribution from the Department of Chemistry (M/C 111), University of Illinois at Chicago, 845 W. Taylor St., Chicago, Illinois 60607, Institute of Organic Chemistry and Biochemistry, Academy of Sciences, Flemingovo nam 2, 16610, Prague, Czech Republic

Received May 17, 1996. Revised Manuscript Received August 7, 1996[⊗]

Abstract: Vibrational circular dichroism (VCD), absorption, Raman, and Raman optical activity (ROA) spectra for the title compound, a cyclic dimer, were measured in non-aqueous solution. The vibrational normal modes are assigned based on the result from *ab initio* force field calculation. Harmonic frequencies and atomic polar tensors for simulation of IR absorption were calculated both on the (Hartree−Fock SCF) HF/6-31G** level and using density functional theory (DFT) methods with the Becke3/LYP hybrid functional. Magnetic transition dipole derivatives were calculated on the HF/6-31G level, and the ROA polarizability tensors were calculated on the HF/4-31G level. Excellent agreement between the DFT calculated and experimental frequencies was obtained without a need for scaling. Furthermore, using the DFT force field, the correct VCD sign and intensity patterns were reproduced as compared to the experimental mid-IR spectra. Reasonable near-IR VCD and mid-IR ROA sign patterns for the intense peaks were also calculated. The excellent agreement for the mid-IR VCD results shows that medium-sized, biologically relevant molecules can have their spectra simulated using quantum mechanical techniques to a high level, certainly one suitable for conformational analyses by direct comparison of theory to experimental results. Comparison of DFT and HF level calculations suggests that the improvement found using DFT methods is primarily due to the force field and not to the intensity parameters. DFT atomic polar tensors were systematically weaker than the HF generated ones. Weak coupling between the subunits of this dimer implies dominance by local interactions which suggests that useful extension of these calculational techniques to larger oligomers might be accomplished by transfer of parameters.

Introduction

Several difficulties arise in an *ab initio* quantum mechanical simulation of vibrational properties of larger molecules, especially those of biomolecular interest. Apart from the obvious computer memory and speed limitations, it could in principle be necessary to employ a higher level of calculation for large molecules than is needed for practical normal coordinate analyses of smaller molecules. If the normal mode ordering is to be predicted reliably by such a calculation, higher precision will be needed to fully interpret vibrational spectra of large biomolecules, for example oligopeptides, due to their higher density of vibrational states. The molecular mechanical force fields widely used for biomolecular conformational studies are not precise enough to provide a basis for vibrational spectroscopic simulations. While for smaller molecules a simple scaling of the *ab initio* harmonic force field obtained at the self consistent field (SCF), Hartree−Fock (HF) level can achieve a reasonable agreement between experimental and theoretical frequencies,[1] recent developments have shown that force fields derived using density functional theory (DFT) and moderately sized basis sets do not need scaling.[2] A similar scaled HF-SCF approach may be misleading when applied to large molecular systems, because of the complicated local mode coupling that can occur, especially for near-degenerate modes typical of biopolymeric molecules.[3] In addition, anharmonic forces can have an unpredictable effect on the vibrational spectra of even the smallest systems, but for larger molecules, low-energy torsions and large-amplitude motions provide a different source of potentially important anharmonicity.

In the light of the difficulties mentioned above, we here present experimental and theoretically simulated vibrational spectra for the (3*S*,6*S*)-3,6-dimethyl-1,4-dioxane-2,5-dione (L-lactide) molecule, a small oligomer (more precisely, a cyclic dilactone) of potential biomolecular interest.[4] Quite remarkably, we were able to predict its spectra within the harmonic approximation to a good level of agreement. Not only were the computed frequencies comparable to those found experimentally, but IR and Raman intensities as well as the vibrational optical activity properties measured using vibrational circular dichroism (VCD)[5−8] and, to a lesser extent, Raman optical activity (ROA)[9−10] could be predicted relatively well with various levels of approximation (i.e. limited basis set computa-

* To whom correspondence should be addressed at UIC.
† University of Illinois at Chicago.
‡ Present address: IPNS Division, Argonne National Laboratory, B-360, 9700 S. Cass Ave. Argonne, IL 60439.
§ Institute of Organic Chemistry and Biochemistry.
⊗ Abstract published in *Advance ACS Abstracts,* October 1, 1996.

(1) Forgarasi, G.; Pulay, P. *Annu. Rev. Phys. Chem.* **1984**, *35*, 8106.
(2) Stephens, P. J.; Devlin, F. J.; Ashwar, C. S.; Chabalowski, C. F.; Frisch, M. J. *Faraday Discuss.* **1994**, *99*, 103. Devlin, F. J.; Stephens, P. J.; Cheeseman, J. R.; Frisch, M. J. *J. Am. Chem. Soc.* **1996**, *118*, 6327. Devlin, F. J.; Finley, J. W.; Stephens, P. J.; Frisch, M. J. *J. Phys. Chem.* **1995**, *99*, 16883. Stephens, P. J.; Devlin, F. J.; Chabalowski, C. F.; Frisch, M. J. *J. Phys. Chem.* **1994**, *98*, 11623. Stephens, P. J.; Ashvar, C. S.; Devlin, F. J.; Cheeseman, J. R.; Frisch, M. J. *Mol. Phys.* In press.
(3) Tavan, P. In *Spectroscopy of Biological Molecules*, Marlin, J. C., Turrell, S., Huvenne, J. P., Eds.; Klumer Academic Publisher: Dordrecht, 1995; p 3.
(4) Kim, H.; Sung, Y. K.; Jung, J.; Baik, H.; Min, T. J.; Kim, Y. S. *Teahan Hwahakhoe Chi* **1990**, *34*, 203.
(5) Stephens, P. J.; Lowe, M. A. *Annu. Rev. Phys. Chem.* **1985**, *36*, 213. Rauk, A. In *New Developments in Molecular Chirality*, Mezey, P. B., Ed.; Kluwer Academic Publisher: Dordrecht, 1991; p 57.
(6) Polavarapu, P. L. In *Vibrational Spectra & Structure*; Bist, H. D., Durig, J. R., Sullivan, J. F., Eds.; Elsevier Science: Amsterdam, 1985; Vol. 13, p 319.
(7) Freedman, T. B.; Nafie, L. A. *Adv. Chem. Phys.* **1994**, *85 (Part 3)*, 207.
(8) Keiderling, T. A. *Appl. Spectrosc. Rev.* **1981**, *17*, 189.

S0002-7863(96)01677-0 CCC: $12.00

tions). This compound belongs to a series of C_2 symmetry[11,12] and related model compounds[13] that we and others[14−17] have studied in an effort to develop procedures for determination of molecular structure on the basis of such optical activity measurement. However, it goes beyond those previous studies in being one of the simplest oligomeric molecules we could study that is closely related (isoelectronic) to the oligopeptide conformational problems of wide interest. As opposed to our earlier simulation of linear polypeptide VCD[18] which relied on computations for idealized dimers without exact experimental analogs, these cyclic dimer calculations can be carried out for precisely the molecule and conformation studied experimentally. Since the lactide has only a single stable conformation which is of C_2 symmetry, calculation of the force fields with higher level basis sets and testing of computed results obtained with various basis sets against relevant spectral data are possible. This is one of the first studies in the vibrational optical activity field to demonstrate the ability to explain both VCD and ROA spectra for a single molecule with a coordinated theoretical approach. Since it is also an oligomer, it provides a model system to explore further application of quantum mechanical methods for stereochemical structural analysis of biopolymeric molecules using vibrational optical activity spectra.

Experimental Section

IR absorption and VCD spectra were measured on an FTIR based spectrometer. In addition, the VCD spectrum of the C═O stretching region was remeasured using a dispersive instrument. The use and construction of these instruments have been discussed and reviewed in the literature.[8,19] The VCD spectrum of the C═O band was obtained using a BaF_2 substrate grid polarizer (Cambridge Physical Sciences), CaF_2 modulator (Hinds), CaF_2 focusing lens, and 2-element array Hg(Cd)Te detector (Infrared Associates) using a monochromator slit width corresponding to ∼10-cm^{-1} resolution. The absorption and VCD spectra in the mid-IR region (1600−800 cm^{-1}) were measured at a resolution of 4 cm^{-1} using an FT-VCD spectrometer (based on a Bio-Rad Digilab FTS-60A FTIR) incorporating a BaF_2 substrate grid polarizer, a ZnSe modulator, a ZnSe focusing lens, and a Hg(Cd)Te detector. VCD spectra in the C−H stretching region were obtained using the same FTIR based spectrometer, but for these, it was operated at a resolution of 8 cm^{-1} to increase the signal-to-noise (S/N) ratio, and a CaF_2 modulator and focusing lens were substituted to increase the near-IR throughput.[20] VCD spectra of the racemic mixture of the lactide were obtained in exactly the same manner and were subtracted from the sample spectra to correct for any baseline irregularities. It might be noted that these C−H stretching VCD spectra are the first new report of near-IR natural VCD obtained on a rapid-scan FTIR-VCD instrument since the initial FT-VCD report of Nafie and co-workers,[21] a measurement which was recently confirmed to be possible with step-scan operation.[20] Since then, it had become a general perception that VCD in the near-IR must be done with a dispersive instrument. Our results show that, with careful signal management, FT-VCD in the near-IR can be done even on a rapid-scan spectrometer.

Raman and ROA spectra of the title compound have also been measured in 180° backscattering geometry using a spectrometer assembled in house.[22,23] This spectrometer consists of an Ar ion laser (Coherent, Innova 300), a spectrograph (ISA J-Y 640), and an intensified diode array detector (PAR 1420 with an OMA III controller). A calcite Glan-laser polarizer (Karl Lambrecht) and an electrooptical modulator (Lasermetrics) were used to produce circularly polarized incident laser light. The laser light is focused through holes in a 45° mirror and in a lens (used to collect the back-scattered light) and onto the sample. After collimating, the back-scattered light passed through a holographic notch filter (Kaiser) and was focused onto the entrance slit of the spectrograph by a camera lens (Nikon). The optical design is a variation of that described by Barron and co-workers.[24] A slit width of 100 μm and a 600-groove/mm grating were used to yield a resolution of 6−8 cm^{-1} for ROA measurements. An 1800-groove/mm grating was used for higher resolution Raman measurements as needed.

Racemic and (3*S*,6*S*)-3,6-dimethyl-1,4-dioxane-2,5-dione (lactide) were purchased from Aldrich Chemicals Co. and used without further purification. Solution samples were prepared by dissolving the lactide in $CDCl_3$. For the mid-IR, solutions with concentrations ranging from 6 (0.03 M) to 2 mg/mL (0.01 M) were placed in a variable path cell (Wilks) with KBr windows set to path lengths of 0.5−0.3 mm and were used for obtaining optimized mid-IR region VCD spectra for bands of different intensities. For the C═O stretch band, a solution in $CDCl_3$ (2 mg/mL or 0.01 M) and a 0.3 mm pathlength were used. Finally, for the C−H stretching region, a $CDCl_3$ solution of 200 mg/mL or 1.15 M concentration was used with a path length of 0.15 mm. For Raman and ROA measurements, a saturated (∼1.2 g in 1.0 mL of $CDCl_3$) solution was placed in a 1 cm × 1 cm quartz cuvette with a polished bottom window through which the laser and the backscattered Raman radiation passed.

Calculational Methods

The X-ray structure of the lactide[25] molecule has, within experimental error, C_2 symmetry with the six-membered ring adapting a boat-like conformation where the methyl groups are held in an equatorial conformation as illustrated in Figure 1. To explore the possibility of identifying alternate conformations, a survey of minimizations starting with other geometries was undertaken with a minimal basis set, but none of these reached a true minimum other than the X-ray determined conformation. In addition, an *ab initio* Hartree−Fock, self consistent field (HF-SCF) energy minimization using a 4-31G basis set was carried out starting from a structure having an initial axial conformation for the methyl groups. This calculation also led to a molecular geometry

(9) Nafie, L. A.; Che, D. *Adv. Chem. Phys.* **1994**, *85 (Part 3)*, 105. Nafie, L. A.; Yu, G.-S.; Qu, X.; Freedman, T. B. *Faraday Discuss.* **1994**, *99*, 13.
(10) Barron, L. D. In *Raman Spectroscopy: Sixty Years On*; Bist, H. D., Durig, J. R., Sullivan, J. F., Eds.; Elsevier Science: Amsterdam, 1989.
(11) Malon, P.; Keiderling, T. A.; Uang, J.; Chickos, J. S. *Chem. Phys. Lett.* **1991**, *179*, 282. Annamalai, A.; Keiderling, T. A.; Chickos, J. S. *J. Am. Chem. Soc.* **1984**, *106*, 6254. Annamalai, A.; Keiderling, T. A.; Chickos, J. S. *J. Am. Chem. Soc*. **1985**, *107*, 2285. Annamalai. A.; Narayanan, U.; Tissot, M.-C.; Keiderling, T. A.; Jalkanen, K.; Stephens, P. J. *J. Phys. Chem.* **1990**, *94*, 194.
(12) Bour, P.; Keiderling, T. A. *J. Am. Chem. Soc.* **1992**, *114*, 9100.
(13) Malon, P.; Mickley, L. J.; Sluis, K. M.; Tam, C. N.; Keiderling, T. A.; Kamath, S.; Uang, J.; Chickos, J. S. *J. Phys. Chem.* **1992**, *96*, 10139. Narayanan, U.; Annamalai, A.; Keiderling, T. A. *Spectrochim. Acta* **1988**, *44A*, 785.
(14) Eggiman, T.; Ibrahim, N.; Shaw, R. A.; Wieser, H. *Can. J. Chem.* **1993**, *71*, 578.
(15) Lowe, M. A.; Stephens, P. J.; Segal, G. A. *Chem. Phys. Lett.* **1986**, *123*, 108. Jalkanen, K. J.; Stephens, P. J.; Amos, R. D.; Handy, N. C. *J. Am. Chem. Soc.* **1987**, *109*, 7193; **1988**, *110*, 2012. Kawiecki, R. W.; Devlin, F. J., Stephens, P. J.; Amos, R. D.; Handy, N. C. *Chem. Phys. Lett.* **1988**, *145*, 411. Stephens, P. J.; Jalkanen, K. J.; Devlin, F. J.; Chabalowski, C. F. *J. Phys. Chem.* **1993**, *97*, 6107. Stephens, P. J.; Chabalowski, C. F.; Devlin, F. J.; Jalkanen, K. J. *Chem. Phys. Lett.* **1994**, *116*, 247. Devlin, F. J., Stephens, P. J. *J. Am. Chem. Soc.* **1994**, *116*, 5003.
(16) Dutler, R.; Rauk, A. *J. Am. Chem. Soc.* **1989**, *111*, 6957. Rauk, A., Yang, D. *J. Phys. Chem.* **1992**, *26*, 437.
(17) Bose, P. K.; Barron, L. D.; Polavarapu, P. *Chem. Phys. Lett.* **1989**, *155*, 423. Bose, P. K.; Polavarapu, P.; Barron, L. D.; Hecht, L. *J. Phys. Chem.* **1990**, *94*, 1734. Black, T. M.; Bose, P. K.; Polavarapu, P.; Barron, L. D.; Hecht, L. *J. Am. Chem. Soc.* **1990**, *112*, 1479. Polavarapu, P.; Hecht, L.; Barron, L. D. *J. Phys. Chem.* **1993**, *97*, 1793. Polavarapu, P.; Black, T. M.; Barron, L. D.; Hecht, *L. J. Am. Chem. Soc.* **1993**, *115*, 7736. Polavarapu, P.; Bose, P. K.; Hecht, L.; Barron, L. D. *J. Phys. Chem.* **1993**, *97*, 11211.
(18) Bour, P.; Keiderling, T. A. *J. Am. Chem. Soc.* **1993**, *115*, 9602.
(19) Keiderling, T. A. In *Practical Fourier Transform Spectroscopy*; Kirshman, J. R., Ferraro, J. R., Eds.; Academic Press: San Diego, 1990; p 203.
(20) Wang, B.; Keiderling, T. A. *Appl. Spectrosc.* **1995**, *49*, 1347.
(21) Nafie, L. A.; Diem, M.; Vidrine, D. W. *J. Am. Chem. Soc.* **1979**, *101*, 496.
(22) Tam, C. N. Ph.D. Thesis, University of Illinois at Chicago, 1995.
(23) Tam, C. N.; Bour, P.; Baumruk, V.; Malon, P.; Keiderling, T. A. In *Proceedings of the 14th International Conference on Raman Spectroscopy*, Hong Kong; Wiley: New York, 1994.
(24) Hecht, L.; Barron, L. D. *Faraday Discuss.* **1994**, *99*, 35.
(25) van Hummel, G. J.; Harkema, S.; Kohn, F. E.; Feuen *Acta Crystallogr.* **1982,** *B36*, 1679.

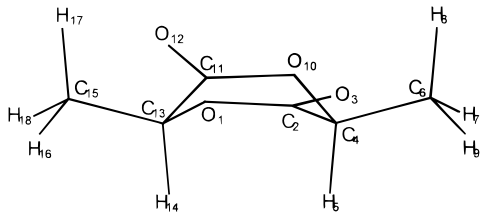

Figure 1. The (3*S*,6*S*)-3,6-dimethyl-1,4-dioxane-2,5-dione molecule, lactide. Arbitrary atom numbering matches Table 1.

characteristic of a transition state with one imaginary vibrational frequency. Hence we feel justified in focusing our effort on the experimental, X-ray determined conformation. The experimental geometry was optimized by an energy minimization, using the CADPAC program package[26] for the HF-SCF calculations and the Gaussian 94 program package[27] for the density functional theory (DFT) calculations. We used the DFT exchange-correlation functional denoted as Becke3LYP (B3LYP)[28] in the Gaussian 94 program, which represents a combination of the Becke hybrid HF-DFT functional[29] with the Lee−Yang−Parr (LYP) correlation functional[30] and has been shown to yield better vibrational spectroscopic properties than the LYP functional alone.[2]

The second derivatives of the energy were calculated analytically to provide the force field (FF) that was used to compute the vibrational frequencies and normal modes. IR intensities could be calculated directly from the atomic polar tensors (APT) evaluated at the DFT-(B3LYP) level. To evaluate the VCD intensities, local atomic contributions to the atomic axial tensor (AAT)[31,32] could be calculated on the HF/6-31G level only due to computer and software constraints. These AATs were combined with the normal coordinates and the APTs from the DFT force following the method previously established by Stephens and co-workers[2] and as has been used in our recent analysis of the VCD of succinic anhydride.[33] To simulate the spectra for comparison to experiment, Lorentzian line shapes of 12 cm^{-1} full width at half height were used.

For Raman intensities the polarizability calculated at the HF/6-31G level was combined with the force field at the DFT(B3LYP) level. ROA spectral intensity parameters[34] could only be calculated on the HF/4-31G level again due to local computer constraints. The electric dipole−electric quadrupole and magnetic dipole−electric dipole polarizability derivatives were calculated with the Cadpac program by use of a one-point numerical differentiation, employing a step size of 0.002 Bohr.

Results

Experimental Spectra. The experimental IR and VCD spectra are shown in Figures 2 and 3 in units of *A* and Δ*A*, as measured. Conversion to molar extinction units can be accomplished by use of the data in the figure captions. The actual spectra were measured for a few different concentrations and all spectra overlapped well when rescaled. In the C−H stretching region, the IR intensities for the fundamental bands of the lactide are very low. Therefore, in addition to the fundamentals, some combination band and overtone bands are also observed as shown in Figure 2a. These may be enhanced

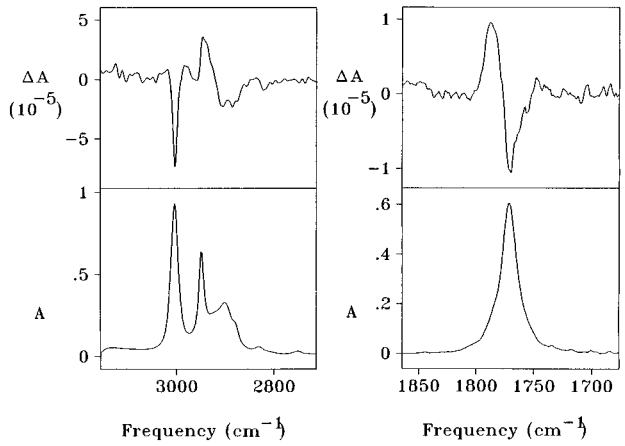

Figure 2. The experimental IR absorption (bottom) and VCD (top) spectra of the lactide in $CDCl_3$ solution over the (a) C−H stretching region (*c* 1.15 M, pl = 0.015 cm) and the (b) C═O stretching region (*c* 0.01 M, pl = 0.03 cm).

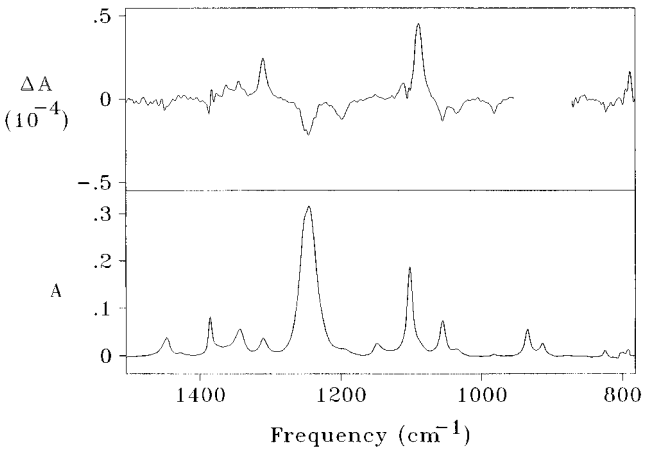

Figure 3. The experimental IR absorption (bottom) and VCD (top) spectra of the lactide in $CDCl_3$ solution over the mid-IR region (overlap of 2 spectra replotted to be equivalent to *c* = 0.01 M, pl = 0.03 cm).

and complicated by the Fermi resonances that can also occur in this region. The VCD of the C−H stretching bands are small in intensity and have a distinctive spectral structure, the two sharper bands giving rise to couplets with the center components partially canceling. The broad negative corresponding to the C_α−H gives the VCD a form much like that seen for the series of amino acids studied by Freedman and co-workers.[35] The VCD for the C═O stretching band consists of an even weaker (in terms of Δ*A*/*A*) couplet, as shown in Figure 2b. Considering its near conservative shape, this VCD couplet presumably arises from the dipolar coupling of the two C═O groups in this nonplanar molecule. The weakness of the C═O stretching VCD is consistent with the near coplanarity of the C═O groups.

In the mid-IR region, a number of relatively more intense (in terms of Δ*A*/*A*) VCD features are observed. Figure 3 shows the experimental mid-IR absorption and VCD spectra of the lactide. It should be noted that there is a small artifact affecting the band at 1385 cm^{-1}, but the overall quality of the VCD spectrum is not affected. There are several intense VCD bands at 1310 (C−H bend, positive), 1249 (C−O stretch, negative), and 1089 cm^{-1} (C−O stretch, positive). The blocked region between 880 and 950 cm^{-1}, which includes the VCD of the IR

(26) Amos, R. D. *CADPAC version 5.0*; SERC Laboratory: Daresbury, UK, 1990.
(27) Frisch, M. J. *GAUSSIAN 94*, Gaussian Inc.: Pittsburgh, PA, 1994.
(28) Becke, A. D. In *The Challenge of d and f electrons*; Salahub, D. R., Zerner, M. C., Eds.; American Chemical Society: Washington, DC, 1989.
(29) Becke, A. D. *J. Chem. Phys.* **1993**, *98*, 5648.
(30) Lee, C.; Yang, W.; Parr, R. G. *Phys. Rev. B* **1988**, *37*, 785.
(31) Stephens, P. J. *J. Phys. Chem.* **1985**, *89*, 748.
(32) Stephens, P. J. *J. Phys. Chem.* **1987**, *91*, 1712.
(33) Bour, P.; Tam, C. N.; Keiderling, T. A.; Shaharuzzaman, M.; Chickos, J. S. *J. Phys. Chem.* In press.
(34) Polavarapu, P. L. *J. Phys. Chem.* **1990**, *94*, 8106. Bose, P. K.; Barron, L. D.; Polavarapu, P. L. *Chem. Phys. Lett.* **1989**, *155*, 423. Bose, P. K.; Polavarapu, P. L.; Barron, L. D.; Hecht, L. *J. Phys. Chem* **1990**, *94*, 1734.
(35) Freedman, T. B.; Chernovitz, A. C.; Zuk, W. M.; Paterlini, M. G.; Nafie, L. A. *J. Am. Chem. Soc.* **1988**, *110*, 6970. Zuk, W. M.; Freedman, T. B.; Nafie, L. A. *J. Phys. Chem.* **1989**, *93*, 1771. Oboodi, M. R., Lal, B. B.; Young, D. A.; Freedman, T. B.; Nafie, L. A. *J. Am. Chem. Soc.* **1985**, *107*, 1547.

Table 1. Optimized and Experimental Geometries of Lactide

coordinate	SCF 6-31G	SCF 6-31G**	B3LYP 6-31G	B3LYP 6-31G**	expl[a]	
bond lengths (Å)						
O1−C2	1.353	1.329	1.381	1.354	1.340	1.341
C2−O3	1.201	1.180	1.225	1.204	1.108	1.201
C2−C4	1.513	1.520	1.524	1.529	1.407	1.507
C4−H5	1.085	1.088	1.100	1.1017	0.976	0.943
C4−C6	1.513	1.514	1.517	1.516	1.494	1.489
C6−H7	1.080	1.083	1.092	1.0921	0.977	0.972
C6−H8	1.080	1.082	1.093	1.0922	0.986	0.968
C6−H9	1.080	1.081	1.093	1.0912	0.929	1.008
O1−O10[b]	2.669	2.685	2.766	2.753	2.725	
bond angles (deg)						
1−2−3	121.2	121.50	120.5	121.0	119.7	119.9
1−2−4	115.0	114.81	115.2	114.9	115.8	116.6
2−4−5	108.3	107.51	108.6	107.8	105.7	105.8
2−4−6	113.6	112.76	113.3	112.7	113.8	114.2
4−6−7	109.3	109.38	109.8	109.9	111.2	109.2
4−6−8	110.2	110.27	110.3	110.3	111.2	108.5
4−6−9	110.1	109.89	109.8	109.6	109.4	111.2
2−1−10	64.4	63.7	62.7	62.6	62.9	62.6
torsional angles (deg)						
1−2−4−5	−84.3	−82.42	−77.7	−78.0	−78.7	−77.1
1−2−4−6	152.5	156.25	158.8	160.4	157.5	158.2
2−4−6−7	180.0	179.81	−179.2	179.5	178.5	176.2
2−4−6−8	−60.1	−60.33	−59.1	−60.2	−65.4	−60.0
2−4−6−9	59.9	59.53	60.3	59.0	55.8	56.2
2−1−10−11	172.7	171.6	175.3	174.9	171.3	171.3
3−2−1−10	162.8	161.5	159.4	159.2	159.1	160.4
4−2−1−10	−18.1	−19.0	−21.2	−20.9	−20.4	−20.1
energy (au)	−531.0708	−531.35157	−534.17807	−534.37169		

[a] From ref 25, since symmetry was not used for the X-ray refinement, the two columns correspond to the two values of that coordinate related by the C_2 symmetry. [b] Nonbonded distance between O_1 and O_{10}, the ester oxygens.

band at 935 cm^{-1}, is obscured by solvent interference. The BaF_2 polarizer used has a cutoff near 800 cm^{-1}, and the MCT detector used is not sensitive beyond that, so that VCD cannot be observed for bands lower than 800 cm^{-1}.

Raman spectra for the whole vibrational region have been measured despite a number of solvent interferences, especially in the low Raman shift region. An ROA spectrum could be easily measured in a region corresponding to the "mid-IR" transitions discussed above where there is little solvent interference. ROA in the low-frequency region is severely hampered by interference from the intense polarized Raman bands arising from the solvent that lead to artifacts which can dominate the spectrum. Figure 4 shows the Raman spectrum after solvent subtraction and the corresponding ROA spectrum in the 750−1550-cm^{-1} region. Complete subtraction of a solvent baseline for the entire Raman spectrum was not possible due to a frequency shift caused by the high concentration of the sample but those bands shown in Figure 4 are not affected by this problem. The ROA spectrum does not require solvent subtraction because the optically inactive solvent gives no detectable baseline deviations beyond the noise in this region. The S/N of the ROA spectrum is reasonable. There are several "couplet-like" features observed at 1330, 1105, and 800 cm^{-1} in addition to a number of single-signed ROA bands. Unfortunately, a substantial artifact was observed in the ROA spectrum for the C═O stretching band preventing us from obtaining useful ROA for this isolated transition.

Calculational Results. A complete set of geometry parameters is given in Table 1, as calculated on the HF-SCF and B3LYP levels, with two basis sets 6-31G** and 6-31G, which can be compared to those parameters resulting from the X-ray crystal structure analysis.[25] The atoms and their interconnections are indicated in Table 1 according to Figure 1. Both the HF-SCF and the DFT/B3LYP energy minimization calculations show a relatively weak dependence on inclusion of polarization functions in the basis set. Little significant difference is notable in the bond length and angle parameters, but some of the torsional angles are better represented with the DFT calculations which include some electron correlation contributions. With the addition of polarization functions to the basis set, the HF-SCF energy decreases by 0.28 au, while the DFT energy decreases only by 0.19 au. Such a relatively weak dependence of the minimum energy on the basis set is rather surprising for an *ab initio* method that includes correlation corrections.[28,36] The hydrogen coordinates cannot be determined by X-ray diffraction as accurately as can the heavy atom coordinates which is one reason for the C−H bonds found experimentally being systematically shorter than those predicted with all the calculations.

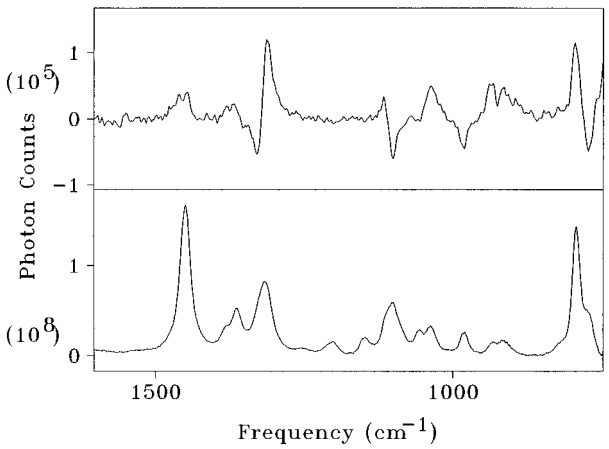

Figure 4. The experimental Raman (bottom) and ROA (top) spectra of the lactide in the mid-IR region (saturated solution in $CDCl_3$).

(36) Pulay, P. *J. Phys. Chem.* **1995**, *99*, 3093.

Table 2. Fundamental Frequencies (cm^{-1}) of Lactide

mode/ symmetry	computed SCF 4-31G	SCF 6-31G	SCF 631G**	B3LYP 6-31G	B3LYP 6-31G**	exptl IR	exptl Raman
1/B	3312	3321	3310	3171	3166	3003	3006
2/A	3312	3321	3310	3171	3166		
3/A	3311	3319	3298	3169	3158		
4/B	3311	3319	3298	3169	3158		
5/A	3226	3231	3218	3082	3076	2949	2949
6/B	3226	3231	3218	3082	3076		
7/A	3210	3217	3193	3038	3014	2897	2905
8/B	3207	3213	3187	3035	3010	2878	2880
9/A	1978	1957	2068	1771	1867	1786	1778
10/B	1968	1947	2056	1766	1861	1771	1765
11/A	1654	1649	1621	1536	1507		1477
12/B	1654	1649	1620	1536	1507	1455	
13/A	1644	1639	1614	1525	1496	1447	1454
14/B	1644	1639	1612	1524	1496	1447	1450
15/A	1593	1589	1561	1463	1427		1380
16/B	1593	1589	1558	1463	1426	1385	1371
17/A	1515	1517	1538	1383	1386		1364
18/B	1505	1507	1521	1378	1374	1343	1333
19/A	1483	1481	1487	1349	1350		1326
20/B	1481	1479	1484	1345	1345	1310	1315
21/B	1381	1382	1425	1226	1274	1249	1253
22/A	1324	1327	1345	1206	1220	1199	1202
23/B	1272	1273	1266	1176	1170	1148	1149
24/A	1251	1252	1271	1144	1134		1109
25/B	1250	1249	1254	1139	1130	1101	1102
26/A	1226	1226	1219	1094	1114	1089	1089
27/B	1184	1186	1180	1073	1072	1055	1054
28/A	1133	1135	1137	1052	1047	1035	1036
29/A	1099	1099	1098	973	995	982	980
30/B	1022	1021	1033	922	945	935	933
31/B	897	898	914	817	829	825	818
32/A	869	865	876	792	801	793	795
33/B	835	832	856	754	774	775	770
34/A	703	702	724	640	655		658
35/B	701	699	704	636	645		644
36/A	656	653	658	600	602	602	605
37/A	509	506	515	469	478	477	479
38/B	502	499	517	464	477	473	
39/A	438	437	446	405	414	419	421
40/A	409	410	408	369	368		369
41/B	363	362	368	332	338		340
42/A	301	298	305	277	282		293
43/B	285	282	285	262	264		
44/B	232	230	245	185	203		224
45/A	226	225	239	175	195		152
46/A	122	123	133	124	129		
47/B	124	124	131	122	128		
48/A	59	59	66	61	64		
a^a	1.108	1.109	1.108	1.039	1.039	(1.000)	
Δ^b [cm^{-1}]	98	100	95	45	50	(0)	
δ^c [%]	6.3	6.3	7.3	3.5	4.2	(0)	

[a] a is the coefficient of the fit $\omega_{calc} = a\omega_{exp}$, where ω_{calc} and ω_{exp} are the calculated and experimental frequencies, respectively, in cm^{-1}. [b] Δ is the absolute mean square deviation between experimental and calculated frequencies. [c] δ is the relative mean square deviation between experimental and calculated frequencies.

Analytical Cartesian second derivatives of the energy evaluated at each calculational level used were used to form a force field and generate frequencies for the fundamental normal modes. As compared in Table 2, the frequencies for the hydrogen stretching modes as derived from the HF-SCF FFs are about 10% higher than the experimental values. For the HF-SCF calculations with simple basis sets (4-31G and 6-31G), the C═O stretching mode frequencies are about 100 cm^{-1} higher than the corresponding experimental ones; but when the polarization basis functions are included, the HF-SCF calculated C═O stretching frequencies deviate even further from experiment. Except for these modes, the HF/6-31G and HF/6-31G** predicted frequencies are similar, with the higher frequency modes being systematically lower and the lower energy modes higher in frequency when the polarization functions are added. There is even less difference between the HF/6-31G and HF/4-31G results, with frequencies differing typically by only a few wavenumbers. On average, the HF-SCF frequencies are about 11% higher than the experimental ones as determined by a fit of the calculated to experimental values as summarized by the coefficient a in Table 2.

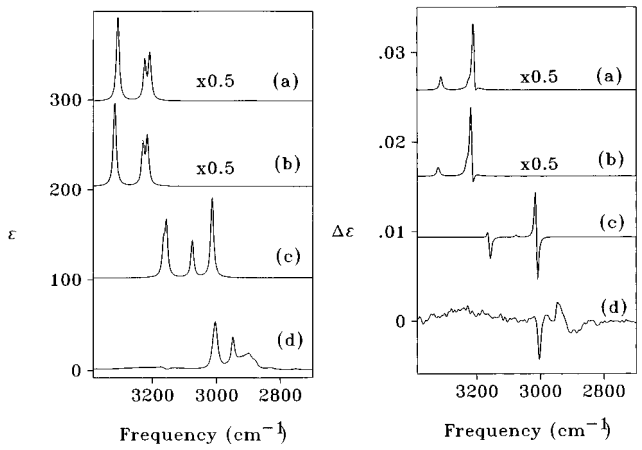

Figure 5. The theoretically simulated and experimental IR absorption and VCD spectra of the lactide in the C−H stretching region. Top to bottom are results from (a) HF/4-31G, (b) HF/6-31G, (c) DFT/B3LYP/631G**, and (d) experiment, respectively, for (left) IR absorption and (right) VCD. HF results are reduced by a factor of 2 for ease of comparison.

In this respect, the DFT method does much better, giving calculated harmonic frequencies on average about 4% higher than those found experimentally. The more conventional measure of vibrational force field quality, the average mean square deviation, Δ, and the relative error, δ, are also reduced by about half as compared to the HF-SCF calculational results (Table 2, bottom). The DFT derived frequencies for the C−H stretching modes are ~150 cm^{-1} high, half the error obtained with the HF-SCF predictions. Using the smaller basis set, B3LYP/6-31G, the DFT predicted C═O stretching frequencies are in excellent agreement with experiment; but with polarization functions added those are about 100 cm^{-1} higher, much as again was seen with the HF-SCF method with the same fundamental basis sets. This improvement with a smaller basis set was unique to the C═O stretch. For purposes of reference, these frequency calculations took 19.7 and 47.7 h for the B3LYP/6-31G and the B3LYP/6-31G** bases, respectively, on an Apollo (HP 700) workstation.

In Figure 5 the experimental IR absorption and VCD spectra for the C−H stretching region are compared to the predicted intensity patterns obtained with each computational level: HF/4-31G, HF/6-31G, and DFT/B3LYP/6-31G**. This is clearly the most difficult spectral region for our calculations. While the improved frequency agreement with the DFT level calculation is striking, the HF intensity patterns are particularly less satisfying having overlapped lower frequency bands and being calculated a factor of 2−4 more intense than observed (which could be a function of the assumed line width). The DFT IR intensity calculation reflects the general characteristics of the three main absorbance maxima, especially if one assumes the lower frequency band, being a mixed contribution of C_α−H stretch with the symmetric CH_3 stretch, has its intensity distributed over combination and overtone bands in some degree of Fermi resonance that effectively serves to broaden the band profile to lower energy. This would also explain why the shoulder seen in the experimental IR absorption bands at 2878

Table 3. Spectral Intensities and Mode Description Using the DFT/B3LYP/6-31G** Force Field

mode/ sym	D^a	R^b	Raman[c] intensity	depolar[d] [%]	ROA[c]/180°	mode description[e]
1/B	11	−232	35	75	−1480	CHs(CH_3)
2/A	4	247	95	72	1350	CHs(CH_3)
3/A	18	−352	87	74	−1440	CHs(CH_3)
4/B	8	320	31	75	1510	CHs(CH_3)
5/A	0	16	207	0	−13	CHs(CH_3)
6/B	19	−13	1	75	23	CHs(CH_3)
7/A	41	125	150	28	65	CHs(C^α)
8/B	4	−123	1	75	−169	CHs(C^α)
9/A	68	1041	27	30	21	C═Os
10/B	1210	−991	3	75	32	C═Os
11/A	4	193	11	75	298	CH_3b(asm)
12/B	10	−107	20	75	−305	CH_3 b(asm)
13/A	30	−331	10	68	−260	CH_3 b(asm)
14/B	14	139	29	75	236	CH_3 b(asm)
15/A	1	−24	3	68	11	CH_3 b(sym)
16/B	72	−73	0	75	−30	CH_3 b(sym)
17/A	0	2	7	42	−35	C^αHb
18/B	105	74	3	75	12	C^αHb
19/A	2	6	5	67	−105	C^αHb
20/B	105	589	8	75	88	C^αHb
21/B	1884	−773	2	75	26	C−Os
22/A	4	−430	3	7	96	ring s
23/B	57	−105	6	75	−82	C^α−CH_3s
24/A	17	660	2	27	15	C^α−Os
25/B	323	−396	5	75	−14	C^α−Os
26/A	27	1580	2	29	11	C−Os
27/B	134	−380	2	75	−28	C−Os
28/A	31	−339	4	64	24	C^α−CH_3s
29/A	11	−63	6	72	−16	C^α−CH_3b
30/B	135	232	0	75	29	C^α−CH_3s
31/B	23	−358	0	75	26	ring def
32/A	14	169	7	23	23	ring def
33/B	42	−493	3	75	−42	ring def
34/A	38	302	15	13	12	breathing
35/B	87	588	0	75	16	ring def
36/A	14	−233	5	54	−57	ring def
37/A	9	86	4	57	−23	C−O−C^α b
38/B	84	1007	2	75	24	C(═O) oop
39/A	1	8	5	35	−15	ring def
40/A	147	−387	1	68	−36	CH_3 b
41/B	154	−564	0	75	−12	CH_3 b
42/A	0	44	2	66	−94	CH_3 b
43/B	70	6	0	75	−52	CH_3 b
44/B	2	3	0	75	−30	CH_3 rot
45/A	8	−38	0	62	−24	CH_3 rot
46/A	1	13	0	74	28	ring b
47/B	7	126	1	75	62	−CH_3 b
48/A	387	4	0	74	−29	ring b

[a] Dipole strength in units of 10^{-4} D^2, where a D $=10^{-18}$ esu·cm in cgs units. [b] Rotational strength in units of 10^{-9} D^2. [c] Arbitrary units for Raman and ROA intensities. [d] Depolarization ratio. [e] For mode assignment: s, stretch, b, bending, oop, out of plane carbon wagging; sym, symmetric; asm, asymmetric.

cm^{-1} is not predicted by the harmonic FF. With the potential impact of anharmonicity taken into account, the DFT computed IR absorption has decidedly the best C−H stretch intensity distribution.

From visual analysis of the motions in each calculated mode, as summarized in Table 3 (column 7), we assign the highest frequency band to an overlap of the asymmetric hydrogen stretches of the methyl groups, calculated at 3166, 3166, 3158, and 3158 cm^{-1}. The experimental VCD corresponding to these four transitions, which cannot be resolved, is predominantly negative, which would agree with the sum of the overlapped DFT calculated *R* values (Table 3, column 3), but not so well with the HF-SCF predicted *R* values (Figure 5b). The positive shoulder seen to low frequency of the main negative experimental VCD feature suggests that the splitting of the CH_3 modes may have been underestimated or that anharmonic effects have some contribution. The very small energy splitting of the two asymmetric CH_3 stretching mode pairs (3166 and 3158 cm^{-1}) results from their being almost totally non-interacting local modes. Indeed, the rotational strengths for the A and B mode in each pair are almost equal in magnitude but opposite in sign (see Table 3), which is consistent with their being weakly coupled dipole oscillators giving rise to nearly canceling rotational strengths.[12,37] Thus the apparently large computed *R* values cannot be realized for the actual VCD of these overlapping bands. This pattern of nearly degenerate vibrational mode pairs is observed for most of the 48 calculated vibrational modes of the lactide, which indicates a low level of interaction across the ring. Such weak coupling implies a dominance of local effects and suggests that calculations on a dimer may provide a useful basis for discussion of spectra for higher oligomers, much as we have seen in our earlier dipeptide calculations.[18,38]

The experimental IR absorption peak at 2949 cm^{-1} corresponds to the symmetric CH_3 hydrogen stretching modes which are calculated to be at 3076 cm^{-1}, and predicted in the DFT result to yield a very small net positive VCD signal after canceling. Again the HF-SCF results are quite different yielding a large net positive VCD. While experimentally the positive VCD is much stronger than that expected from the DFT results corresponding to the CH_3 frequencies, this may be due to mixing with the lower energy modes. It should be noted that the symmetric CH_3 stretch normally can have strong mixing with the overtones of the CH_3 asymmetric deformation modes. The lower energy C_α−H stretching peak (experimentally at 2897 cm^{-1}, calculated 3014/3010 cm^{-1}), by comparison, has the least degeneracy in this region, possibly due to the interaction with the ring C−O modes. This lack of degeneracy is the source of the predicted couplet VCD shape in the DFT results (Figure 5) which again can be seen to be consistent with the experimental VCD spectrum if one assumes mixing with the symmetric CH_3 coordinates and if anharmonic interactions with the CH_3 combination and overtone bands lead to dispersal of the C−H rotational strengths over the 2949- and 2897-cm^{-1} bands. Perhaps future calculations incorporating anharmonic corrections[33,38] can test these assumptions, but for now they are beyond our capabilities with this molecule.

The experimental and computed (HF-SCF and DFT) IR absorption and VCD spectra for the mid-IR region including the C═O stretching modes exhibit much clearer agreement as compared in Figures 6 and 7, respectively, for the same set of calculations. The DFT calculated absorbance spectrum (Figure 6c) is in somewhat better agreement with experiment than that obtained at the HF-SCF level, in that it better reproduces the frequencies and, hence, the relative pattern of IR intensities in the experimental spectrum. However, variations in the relative intensity patterns between these calculated mid-IR spectra is minor except for the region from 1000 to 1250 cm^{-1} which tends to be assigned to C−C and C−O (ring) stretches (Table 3).

As shown in Figure 7, the VCD sign pattern and intensity distribution is in strikingly good agreement with the experimental results, and is virtually the same in all three calculations if one accounts for frequency shifts. This indicates that, for the lactide, the real gain in VCD spectral simulation accuracy from using DFT level calculations is small if the axial tensor is still evaluated at the HF-SCF level. Furthermore, there is little improvement in the AAT in going from the 4-31G to 6-31G

(37) Holzwarth, G.; Chabay, I. *J. Chem. Phys.* **1972**, *57*, 1632.
(38) Bour, P.; Sopkova, J.; Bednarova, L.; Malon, P.; Keiderling, T. A. *J. Comput. Chem.* submitted for publication. Bour, P. Ph.D. Thesis, Acad. Sci. Czech. Rep., Prague, 1993.

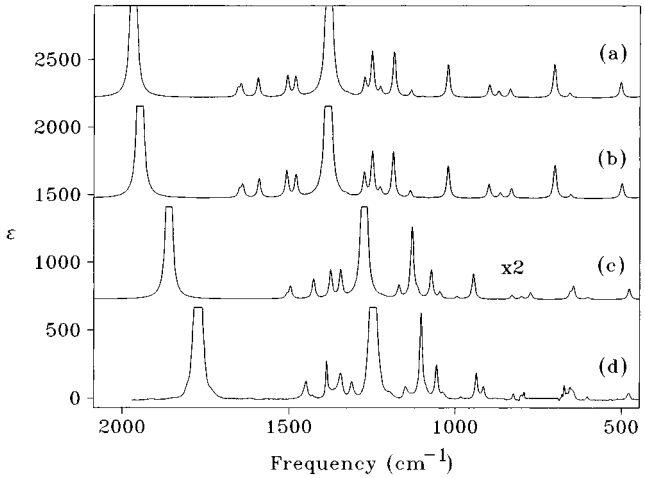

Figure 6. The theoretically simulated and experimental IR absorption spectra of the lactide in the mid-IR. Top to bottom are results from (a) HF/4-31G, (b) HF/6-31G, (c) DFT/B3LYP/631G**, and (d) experiment, respectively. The 700−800-cm^{-1} region is not shown due to solvent interference. DFT results are increased by a factor of 2 for ease of comparison.

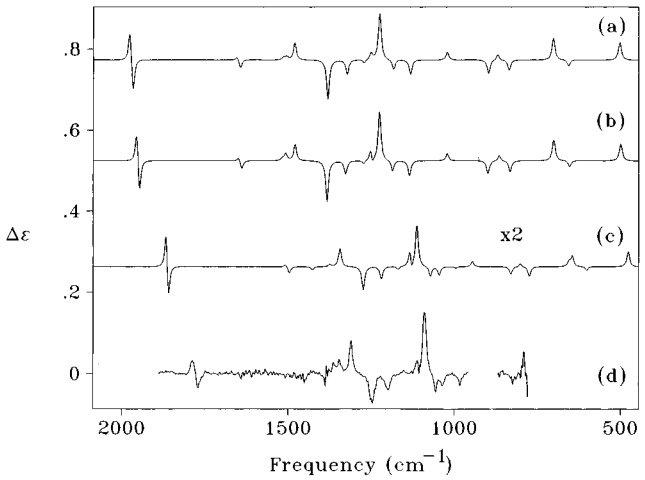

Figure 7. The theoretically simulated and experimental VCD spectra of the lactide in the mid-IR. Top to bottom are results from (a) HF/4-31G, (b) HF/6-31G, (c) DFT/B3LYP/631G**, and (d) experiment, respectively. The 850−900-cm^{-1} region is not shown due to solvent interference. DFT results are increased by a factor of 2 for ease of comparison.

basis sets. Unfortunately computation of the AAT with larger basis sets having polarization functions was not possible at this time. Improved representation of the vibrational frequencies remains the main strength of the DFT approach in this comparison. Noting that both the computed VCD and absorption spectra are ∼2 times less intense than the experimental spectra, it would seem that the APT values are not improved with DFT-level calculation. The exceptional quality of these calculated results includes the C═O stretches, whose VCD and absorption are characteristic of coupled oscillator VCD.[17,37] The high aborption intensity difference (nearly 20 times) in the A and B symmetry C═O modes arises from these groups being only somewhat deviated from a colinear geometry. Quantitative comparison of theory and experiment in terms of *R* and *D* values is not possible due to spectral overlap. However, presentation of both experimental and simulated spectra in terms of molar extinction units in the Figures 5−7 does allow a quantitative assessment of the result.

The Raman and ROA spectra are compared to their theoretical simulations using the HF-SCF and DFT force fields in Figures

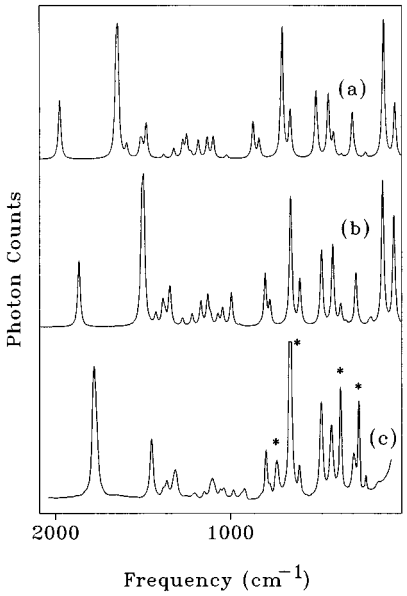

Figure 8. The theoretically simulated and experimental Raman spectra of the lactide. Top to bottom are results from (a) HF/4-31G, (b) DFT/B3LYP/631G** + HF/6-31G polarizability tensors, and (c) experiment, respectively. The residual Raman bands after subtraction of the $CDCl_3$ solvent are marked by asterisks.

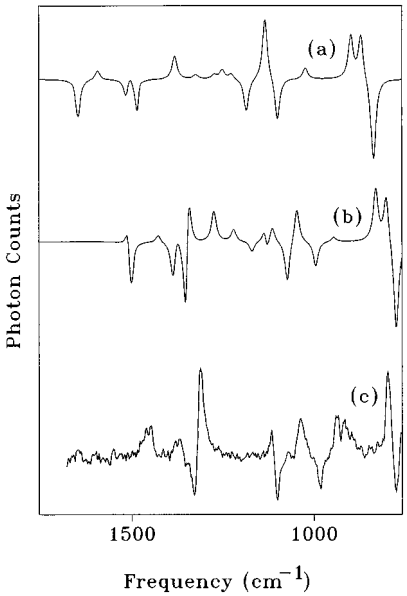

Figure 9. The theoretically simulated and experimental ROA spectra of the lactide. Top to bottom are results from (a) HF/4-31G, (b) DFT/B3LYP/631G** + HF/4-31G polarizability tensors, and (c) experiment, respectively.

8 and 9, respectively. The solvent interferences in the full (down to ∼100 cm^{-1}) experimental Raman spectrum (Figure 8c) cannot be completely subtracted because the solvent band frequencies shifted due to the high concentration of the lactide solution used. The affected bands are marked with asterisks; all fall below the region used for ROA (Figures 4 and 9). In the region between 700 and 1650 cm^{-1}, *qualitative* agreement between the ROA and Raman spectral patterns and the simulated spectra can be observed in both calculations, although the calculated intensities much less obviously parallel the experimental ones than found above for the VCD and IR absorption intensities. In particular, the ROA signs and relative intensities of the intense couplets at ∼1350, 1100, 970−1050, and 800 cm^{-1} are simulated correctly (Figure 9), but some additional/incorrect bands are computed with substantial intensity at ∼1500, 1270,

and 850 cm^{-1}. Presumably, the parallel of HF-SCF and DFT results in Figure 9 is due to the difference between them being only the FF used and not the polarizability derivatives, because only the HF/4-31G derived polarizability derivatives were used for both sets of ROA calculations. Neglecting the higher level corrections to the polarization derivatives probably limits the accuracy of calculating the Raman tensors more than it does for the atomic axial tensors used in IR and VCD calculations. In particular, the asymmetric CH_3 deformation motions in the lactide molecule, whose frequencies are around 1450 cm^{-1}, have much more intense Raman and ROA intensities (wrong sign even!) for the computational as compared to the experimental results. The ROA signal of these CH_3 deformation modes is positive, but weak, as opposed to the strongly negatively biased couplet found in the DFT and HF-SCF calculations. For the symmetric CH_3 deformation modes, an intense positive ROA couplet is seen and also found in the DFT calculations but is poorly simulated by the HF-SCF level calculations. The fingerprint region ($\sim$1200 to 900 cm^{-1}) has the best qualitative agreement between theory and experiment for the most intense features after accounting for frequency shifts due to the two force fields.

Discussion

Density functional theory is a recently exploited theoretical approach for calculating *ab initio* geometries, energies, and force fields that can partially compensate for configuration interaction effects in a much more computationally efficient manner than with conventionally used perturbation (e.g. MP2) methods. This increased efficiency allows one to compute force fields and intensity parameters at a moderately high accuracy for even larger molecules than was before possible. For these reasons, it is now viewed as being superior to the conventional Hartree−Fock-SCF methods,[28] but it should be recognized that the density functional is a parametrized component on which the calculation can depend strongly and not necessarily in a systematic manner.[28] Recently, the DFT method has been successfully exploited for VCD calculations.[2,33] The added accuracy of the DFT method for force field determination (with the B3LYP functionals) has a further impact on studies of larger oligomeric molecules such as the cyclic dimer, lactide. Our results show that DFT frequency and APT determination coupled with HF level AAT evaluation may be a reasonable method for interpretation of the biopolymer VCD problem, but they also suggest that HF APT and AAT values may suffice provided one can generate a force field accurate enough to give reasonable frequencies.

The comparison between the HF-SCF and DFT approaches for calculating VCD and ROA spectra, shown in Figures 5−9, is consistent overall with our expectation that the DFT method gives better results due to the much improved representation of the experimental vibrational frequencies. These might be even more improved with a reasonable accounting for the effects of anharmonicity as we have described above for the C−H stretching VCD. Surprisingly, the relative VCD intensities in the mid-IR are quite comparable in sign pattern and rough magnitude for the three simulations (Figure 7), differing mainly in frequency dispersion. Thus the lactide could be seen as a case where VCD is less sensitive than the absorbance to improvement in the level of calculation. We have seen this behavior in other systems[11,13] and attribute it to the VCD having a strong dependence on the relative geometry of interacting local dipoles induced in the normal mode arising from the dependence of the rotational strength on the scalar product of the electric ($\boldsymbol{\mu}$) and magnetic ($\mathbf{m}$) transition dipole moments, $R = \mathrm{Im}(\boldsymbol{\mu}\cdot\mathbf{m})$. Thus errors in the APTs and AATs are somewhat modulated by geometrical parameters in VCD measurements, but these errors are more important in IR absorption simulation due to the relative lack of such geometrical constraints in determination of the dipole strength ($D = \boldsymbol{\mu}\cdot\boldsymbol{\mu}$). Similarly, the experimental ROA pattern was better reproduced by the DFT than the HF-SCF calculations due to the superior FF obtained with the DFT, there being no change in the intensity parameters for the ROA simulation.

It was not possible to compare the DFT and MP2 methods of accounting for configuration interaction for the lactide molecule because MP2 calculations with these same basis sets for this "relatively large" molecule are not possible with our computer resources. This is an advantage of the more efficient DFT approach. Using the same basis set size (6-31G**), the DFT and MP2 approaches were shown to yield comparable results in our VCD calculation for *trans*-dideuteriosuccinic anhydride.[33] To be fair, it must be made clear that the atomic axial tensors in both of our computations were calculated at the HF-SCF level only for VCD simulation and all the Raman tensors were also obtained at that level. Thus force field and APTs are the primary input differences distinguishing the DFT computations from the HF-SCF ones in this test. Previous studies by Stephens and co-workers also indicated similar conclusions.[2,39]

The lactide molecule is a nonplanar heterocyclic six-membered ring. It is isoelectronic to the cyclic dipeptide, *cyclo*-(L-Ala-L-Ala), a molecule of more obvious potential biological interest. However, this analogous diketopiperazine-type molecule is nearly planar. As a consequence, its VCD intensities are much weaker than for the significantly nonplanar, boat conformation, lactide molecule. In a series of tests, we have not been able to measure VCD for the *cyclo*-(L-Ala-L-Ala) and have only obtained significant VCD signals for proline containing diketopiperazines which, due to the pyrrole ring, are much less planar.[40] On the other hand, cyclic tri- and higher oligopeptides give rise to significant VCD effects due to the increased conformational flexibility allowed by the larger ring;[41,42] and, of course, long-chain oligomeric peptides give rise to significant and conformationally useful VCD spectra.[43,44] One of our original purposes was to examine the use of vibrational optical activity to establish the stereochemical configuration of the related cyclic peptides using the lactide molecule as a model. Work is in progress toward this direction. Our recent work has demonstrated the feasibility of propagating FF and APT and AAT parameters calculated for dimeric molecules onto a polymeric framework in order to better simulate the IR and VCD spectra of larger molecules.[38] The successful results shown here for the lactide imply that DFT based FF calculations will provide a more reliable basis for such extensions. However, our results also indicate that continued computation of the AAT at the HF level, even with smaller basis sets such as 6-31G, can be a reasonable approximation

(39) Cheeseman, J. R.; Frisch, M. J.; Devlin, F. J.; Stephens, P. J. *Chem. Phys. Lett.* **1996**, *252*, 211. Devlin, F. J.; Bak, K. L.; Taylor, P. R.; Stephens, P. J. *J. Phys. Chem.* **1996**, *100*, 9262.

(40) Silva, R. G. A. D.; Keiderling, T. A. Unpublished results.

(41) Xie, P.; Zhou, Q. W.; Diem, M. *J. Am. Chem. Soc.* **1995**, *117*, 9502. Xie, P., Diem, M. *J. Am. Chem. Soc.* **1995**, *117*, 429.

(42) Malon, P.; Yoder, G.; Lebl, M.; Keiderling, T. A. Unpublished results.

(43) Keiderling, T. A.; Pancoska, P. In Advances in Spectroscopy. *Biomolecular Spectroscopy Part B*; Hester, R. E., Clarke, R. J. H., Eds.; John Wiley: Chichester, 1993; Vol. 21, p 267. Keiderling, T. A. In *Circular Dichroism and the Conformational Analysis of Biomolecules*; Fasman, G. D., Ed.; Plenum: New York, 1996; p 555.

(44) Freedman, T. B.; Nafie, L. A.; Keiderling, T. A. *Biopolymers (Peptide Science)* **1995**, *37*, 265.

for such oligomers. The increased computational efficiency of the DFT approach will also allow one to more realistically simulate side chain effects on the model dimeric unit.

This paper is an extension of our ongoing development of applications for VCD and ROA as a probe for stereochemistry using theoretical simulation of the spectra to test structural models. Our previous studies have focused on 3-, 4-, and 5-membered-ring molecules with increasing complexity of the hetero-atoms. Of most direct relevance to the lactide, the previously studied γ-butyrolactone molecule provided an unduly complex system because of the flexibility of its 5-membered ring[13] while four-membered oxygen-containing rings yield straightforwardly interpretable spectra.[2,14] The results shown here clearly demonstrate that the theory convincingly agrees with the experiment for this six-membered-ring molecule with one stable conformation. In other studies of six- and four-membered-ring systems where the conformation was relatively fixed, the agreement of computed and experimental VCD has been similarly high.[14,17] Previous ROA studies have tended to focus on smaller molecules.[34] The quality of agreement found here, considering the limited basis set used for evaluating polarizability derivatives, can be viewed as acceptable. Certainly the ROA calculations are good enough to distinguish between optical enantiomers. Should it be a question, the absolute configuration of the lactide molecule can be said to be established by VCD and is consistent with what is observed by X-ray diffraction and deduced from its synthetic preparation.[25] These results then further show that vibrational optical activity (VCD and ROA) is useful for obtaining absolute stereochemical information for medium sized molecules where at least a reasonable level of *ab initio* theory (DFT) is still practicable.

Acknowledgment. This work was supported in part by a continuing grant from NIH (GM 30147), an NSF International co-operation grant (INT 91-07588), and one from the Grant Agency of the Czech Republic (203/95/0105). We thank Prof. James Chickos for suggesting study of lactide, Dr. Jana Sopkova for discussion of the X-ray structure and Prof. Philip Stephens for preprints of unpublished work. Computational facilities of the Department of Chemistry, University of Illinois at Chicago, and at the Institute of Organic Chemistry and Biochemistry, Academy of Sciences of the Czech Republic, were provided for these calculations. C.N.T. would like to thank Mrs. Philip L. Hawley for the Philip L. Hawley Fellowship administered through the University of Illinois at Chicago.

JA961677I